analytical chemistry

Article

pubs.acs.org/ac

Visualization of Endoplasmic Reticulum Aminopeptidase 1 under Different Redox Conditions with a Two-Photon Fluorescent Probe

Shuai Xu,[†,§] Hong-Wen Liu,[†,§] Xiao-Xiao Hu,[†] Shuang-Yan Huan,[*,†] Jing Zhang,[†] Yong-Chao Liu,[†] Lin Yuan,[†] Feng-Li Qu,[*,‡] Xiao-Bing Zhang,[*,†] and Weihong Tan[†]

[†]Molecular Science and Biomedicine Laboratory, College of Chemistry and Chemical Engineering and College of Biology, State Key Laboratory of Chemo/Biosensing and Chemometrics, Collaborative Innovation Center for Chemistry and Molecular Medicine, Hunan University, Changsha 410082, P.R. China

[‡]The Key Laboratory of Life-Organic Analysis, College of Chemistry and Chemical Engineering, Qufu Normal University, Qufu, Shandong 273165, P.R. China

Supporting Information

ABSTRACT: Endoplasmic reticulum aminopeptidase 1 (ERAP1), a metallopeptidase belonging to the M1 peptidase family, plays an important role in antigen processing in vivo. Additionally, many diseases are caused by ERAP1 perturbation. Thus, an efficient method for monitoring its content is extremely important for disease diagnosis and treatment. However, few fluorescent probes have been reported for efficiently monitoring ERAP1 in living cells and tissues. In this work, a two-photon fluorescent probe (**SNCL**) containing 1,8-naphthalimide (two-photon fluorophore), L-leucine (trigger moiety), and a methyl sulfonamide moiety (endoplasmic reticulum-targeting group) for imaging ERAP1 activity in living cells is reported for the first time. The optimized probe exhibited high sensitivity toward ERAP1, with about a 95-fold fluorescence enhancement at 550 nm. Herein, we monitored ERAP1 with **SNCL** by introducing interferon-γ to induce ERAP1 activity in living cells. The content of ERAP1 was dependent on the redox state of the endoplasmic reticulum, which was demonstrated by using **SNCL** to monitor the enzymatic activity of ERAP1 under different redox conditions. Excitingly, **SNCL** was also successfully applied for monitoring ERAP1 in tumor tissue with an imaging depth of 50−120 μm. In conclusion, **SNCL** not only can be used for the sensitive detection of endogenous ERAP1 in living cells and tumor tissues but also can serve as a potentially useful tool to reveal ERAP1-related diseases.

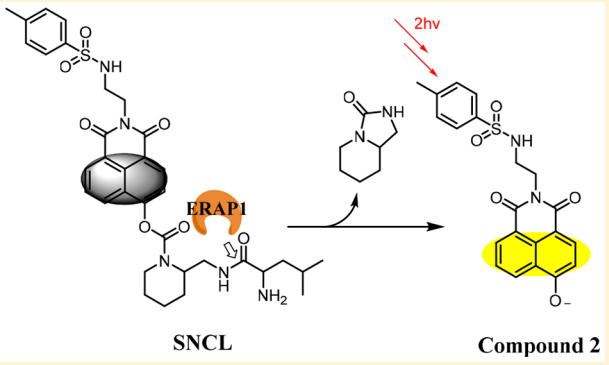

Endoplasmic reticulum aminopeptidase 1 (ERAP1) was once named adipocyte-derived leucine aminopeptidase (A-LAP)[1,2] or puromycin-insensitive leucyl-specific aminopeptidase (PILS-AP)[3] before it was isolated from the lumen of the endoplasmic reticulum (ER) and renamed by Saric in 2002 based on its location.[4] As reported, ERAP1 can participate in optimizing peptides that serve as targets for cytotoxic T cells during infection and disease.[5,6] Thus, disturbed expression of ERAP1 may cause improper antigen processing, leading to the escape of the tumor from immune surveillance.[7] Moreover, ERAP1 also plays an important role in regulating blood pressure.[8] After being released from the ER, plasma angiotensin II, a blood pressure-related peptide, will be digested by ERAP1, resulting in decreased blood pressure. Given the above illustration, it is necessary to develop effective chemical tools to monitor ERAP1 activity to better understand pathophysiological processes.

As powerful tools, fluorescence probes have been widely applied for the detection of different enzymes in human biological processes because of their virtues of allowing fast analysis and high temporal−spatial resolution.[9−12] In the traditional method for monitoring ERAP1 activity, leucine-7-amino-5-methylcoumarin (L-Amc) is used as the fluorogenic aminopeptidase substrate, which was initially employed by Masafumi Tsujimoto.[1] However, ERAP1 had to be extracted from cells with compromised membranes for this method, which was time-consuming and laborious. To the best of our knowledge, no efficient fluorescent probe has been designed for directly imaging ERAP1 activity in living cells, which limits the investigation of this pivotal enzyme. Furthermore, traditional fluorescent probes that work with one-photon microscopy are not favorable for deep-tissue imaging,[11] which limits their biological applications. Two-photon (TP) fluorescence probes, which are excited by two near-infrared photons, have been developed for the detection of various biorelated targets.[13−22] Although two-photon probes possess some drawbacks, such as photobleaching and photodamage to biosamples caused by the high photon density,[23,24] they have the ability to realize deeper

Received: April 27, 2017
Accepted: June 14, 2017
Published: June 14, 2017

DOI: 10.1021/acs.analchem.7b01561
Anal. Chem. 2017, 89, 7641−7648

tissue imaging, better three-dimensional spatial localization, and higher imaging resolution, which make them an attractive candidate for imaging various biotargets.[25]

In this work, a two-photon fluorescent probe (**SNCL**) was designed and synthesized for imaging ERAP1 activity in a biological system for the first time. **SNCL** was designed on the basis of the principle of intramolecular charge transfer (ICT) by modifying the C-4 phenol group into a relatively electron-poor carbamate in order to yield a change in its emission upon reaction with the target enzyme. A 4-hydroxy-1,8-naphthalimide derivative was chosen as the two-photon fluorophore owing to its outstanding spectroscopic properties, such as high photostability and large two-photon absorption cross-section.[10,26−28] L-Leucine was selected as the trigger moiety because it is rich in the hydrophobic substrates that ERAP1 prefers to bind.[29] A methyl sulfonamide moiety was selected as the ER-targeting group,[30,31] which localizes the probe to the ER rapidly after its internalization. In the basic skeleton, a tertiary carbamyl linked via 1,2-diamine-based cyclization was selected as the spacer to construct a quick response system.[32−34] As shown in Scheme 1, ERAP1 could cleave the leucine group of **SNCL** to release the cyclic urea and the fluorophore part (compound **2**), resulting in fluorescence recovery. **SNCL** was further optimized to be applied in complex biological systems, and the results showed that **SNCL** could be used to detect ERAP1 in living cells and tissues. In this design, compound **NCL** was chosen as a control probe.

Scheme 1. Responses of SNCL and NCL to the Target Enzyme

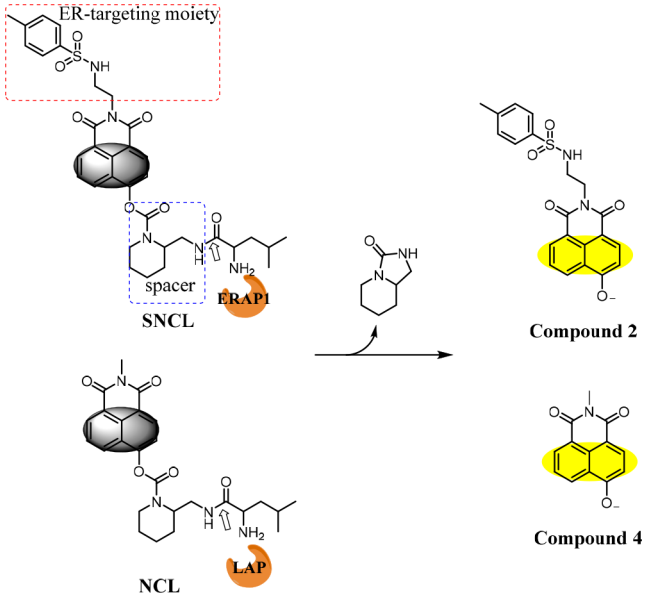

EXPERIMENTAL SECTION

Reagents and Apparatus. All chemicals were obtained from commercial suppliers and used without purification. Leucine aminopeptidase (LAP, microsomal from porcine kidney) and bestatin were purchased from Sigma-Aldrich and Heowns, respectively. Ultrapure water was used to prepare all samples. Fluorescence and absorption spectra were measured with a Fluoromax-4 spectrofluorometer (HORIBA Jobin Yvon) and a UV−vis spectrophotometer (Shimadzu UV-2550, Japan), respectively. The pH measurements were recorded on a Mettler-Toledo Delta 320 pH meter. ^{1}H and ^{13}C NMR spectra in DMSO-d_6 were recorded on a Bruker DRX-400 spectrometer (Bruker) system. Mass spectra were recorded using an LCQ Advantage ion trap mass spectrometer (Thermo Finnigan). Silica gel (200−300 mesh) was used for column chromatography and obtained from Qingdao Ocean Chemicals (Qingdao, China). One- and two-photon fluorescence imaging experiments were recorded by an Olympus FV1000-MPE multiphoton laser scanning confocal microscope (Olympus, Japan). **SNCL** and **NCL** were synthesized as shown in Schemes 2 and S1, respectively, and they were characterized by ^{1}H NMR, ^{13}C NMR, and MS (see the Supporting Information).

Synthesis of SNCL. To a solution of compound **2** (0.41 g, 1.0 mmol) and triphosgene (0.89 g, 3.0 mmol) in dry CH_2Cl_2 (15 mL) was added DIPEA (0.5 mL), and the solution was stirred at 0 °C for 1 h. The reaction was allowed to stir overnight at room temperature. The mixture was then evaporated to dryness under reduced pressure, and the volatiles were trapped and neutralized with a sodium hydroxide solution. To the solid residue was added compound **3** (0.2 g, 0.6 mmol)[35] in dry CH_2Cl_2 (15 mL) dropwise, followed by DIPEA (0.5 mL). After 10 h of stirring at room temperature, the reaction mixture was then concentrated under reduced pressure to obtain the solid residue. The solid was redissolved in CH_2Cl_2/TFA and stirred at room temperature for 3 h. Then, the solvent was evaporated, and the residue was purified by silica gel chromatography with CH_2Cl_2/MeOH (50:1) to obtain **SNCL** (235 mg, 35%). ^{1}H NMR (400 MHz, DMSO-d_6)

Scheme 2. Synthesis Route for SNCL

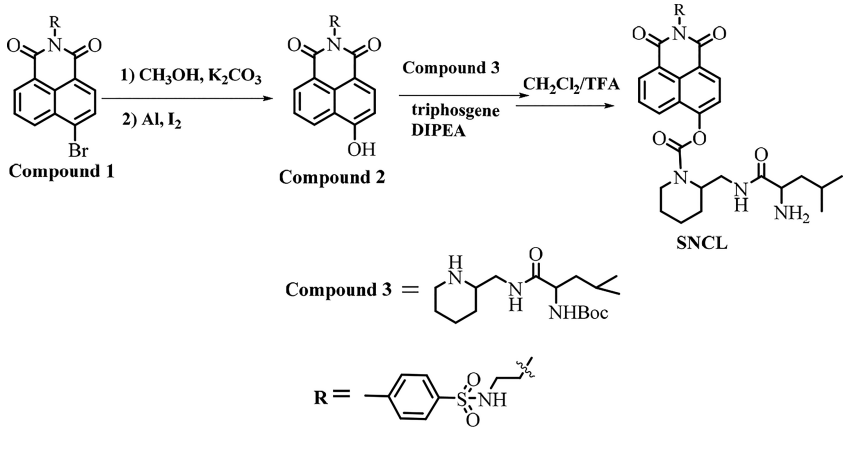

DOI: 10.1021/acs.analchem.7b01561
Anal. Chem. 2017, 89, 7641−7648

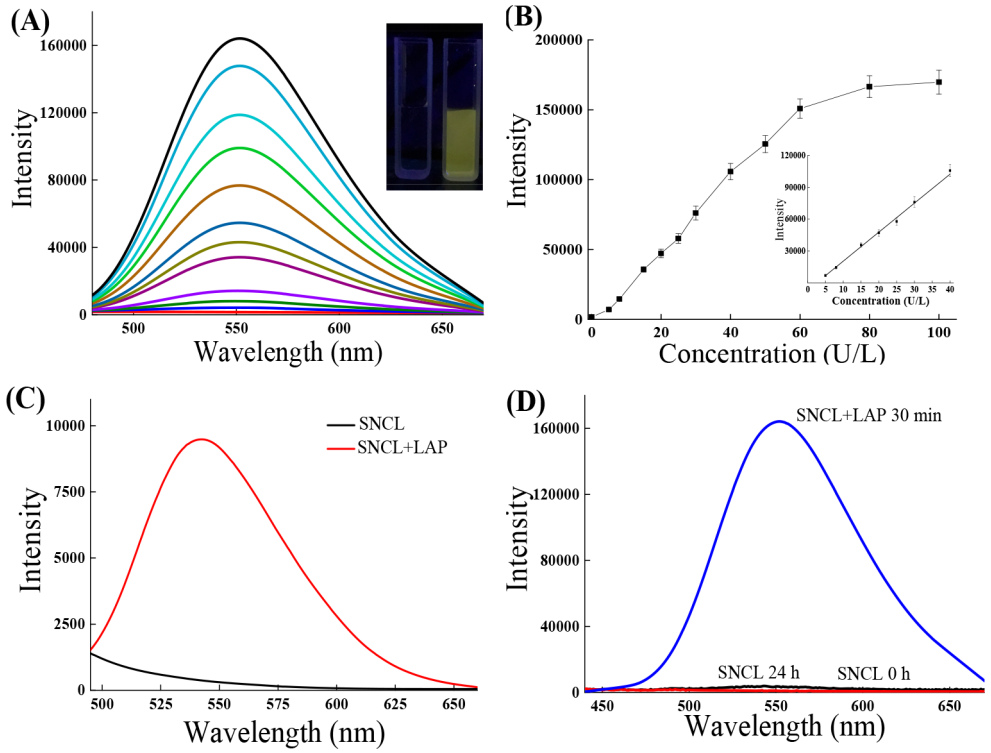

Figure 1. (A) Emission spectra of **SNCL** (10 μM) after reacting with various concentrations of LAP for 30 min. (B) Calibration curve of **SNCL** (10 μM) with LAP. The inset shows the linear relationship between the concentration of LAP and the fluorescence emission at 550 nm. (C) Two-photon excited emission spectra of **SNCL** in the absence and presence of LAP (λ_{ex} = 820 nm). (D) Emission spectra of **SNCL** alone in buffer solution (pH 7.4) for 0 h (red) and 24 h (black) and in the presence of LAP (blue).

δ 8.51−8.40 (m, 3H), 7.90 (d, J = 8.1 Hz, 1H), 7.70 (dd, J = 9.3, 6.8 Hz, 1H), 7.61 (d, J = 7.9 Hz, 2H), 7.24 (d, J = 7.8 Hz, 2H), 4.12 (t, J = 6.6 Hz, 2H), 3.60 (d, J = 7.6 Hz, 2H), 3.49−3.37 (m, 2H), 3.34−3.24 (m, 2H), 3.10 (t, J = 6.7 Hz, 2H), 2.27 (s, 3H), 1.82−1.60 (m, 7H), 1.33 (m, 2H), 0.79 (d, J = 6.3 Hz, 6H). ^{13}C NMR (101 MHz, DMSO-d_6) δ 175.34, 163.86, 163.32, 152.64, 142.92, 138.08, 131.74, 131.46, 129.92, 128.99, 128.77, 127.89, 126.82, 125.53, 122.73, 119.78, 119.49, 53.27, 51.44, 49.05, 44.05, 43.73, 38.18, 26.45, 25.71, 25.33, 24.39, 23.54, 22.16, 22.10, 21.33. MS m/z [(M + H)$^+$]: 664.2.

Spectrophotometric Experiments. Fluorescence and absorption spectra were both measured in a buffered aqueous DMSO solution (10 mM PBS, pH = 7.4, DMSO/H_2O = 1:19, v/v). Samples were excited at 420 or 820 nm, and the emission wavelength was from 470 to 670 nm. The final test solution of **SNCL** (10 μM) was obtained by mixing 10 μL of **SNCL** stock solution (1×10^{-3} M) in DMSO with 0.99 mL of various analyte buffer/DMSO solutions. The enzyme was incubated with **SNCL** in vitro at 37 °C for 30 min before recording the absorbance or fluorescence spectra, with both excitation and emission slits set at 3 nm. The control groups were prepared and measured under the same conditions. The TP excited fluorescence intensity was measured at 730−860 nm using Rhodamine B as the reference. **SNCL** was dissolved in a PBS/DMSO buffer solution (10 mM PBS, pH = 7.4, DMSO/H_2O = 1:19, v/v); then, the intensities of the TP excited fluorescence spectra of **SNCL** and the reference with the same excitation wavelength were recorded. The TP absorption cross-section (δ) was calculated as follows

$$\delta = \delta_r(S_s\Phi_r\phi_rC_r)/(S_r\Phi_s\phi_sC_s) \quad (1)$$

where the subscripts s and r refer to the sample and reference, respectively.[36,37]

Cytotoxicity Study. The cytotoxicities of **SNCL** and **NCL** were evaluated by CCK-8 assays. HeLa cells were seeded at 1×10^5 cells per well in 96-well plates and cultured for 24 h before treatment, followed by exposure to different concentrations (2−20 μM) of **SNCL** or **NCL** for 24 h. Then, the culture media was removed and the wells were washed with DPBS (200 μL). CCK-8 was added to each well, and the cells were incubated at 37 °C for 1 h. The absorbance at 450 nm was measured with a microplate reader.

Two-Photon Fluorescence Microscopy Imaging of ERAP1 in Living Cells. HeLa cells were washed with DPBS before being incubated with **SNCL** (10 μM) at 37 °C for 30 min (in DPBS containing 2% DMSO) and then washed with DPBS three times. TP fluorescence microscopy images of HeLa cells were then captured with a mode-locked titanium-sapphire laser source set at a wavelength of 820 nm, and the emission wavelength was recorded at 470−540 nm.

Two-Photon Fluorescence Imaging of ERAP1 in HeLa Tumor Tissue Slices. Five-week-old male BALB/c nude mice were obtained from SJA Co., Ltd. (Changsha, China). HeLa cells (2×10^7 in 100 μL of DPBS) were injected into the left upper extremity of the mice, and frozen tissue slices were prepared from the tumor 6 weeks after the injection. Frozen tissue slices were incubated with 50 μM **SNCL** at 37 °C for 1 h and then washed with DPBS three times before taking TP fluorescence microscopy images. The control samples were pretreated with 2 mM bestatin at 37 °C for 2 h and were then treated with 50 μM **SNCL** at 37 °C for 1 h before imaging.

DOI: 10.1021/acs.analchem.7b01561
Anal. Chem. 2017, 89, 7641−7648

RESULTS AND DISCUSSION

Design of SNCL. In recent years, a few of fluorescent probes have been designed that have revealed the important roles of LAP in living cells.[34,35,38−46] However, ERAP1, as a LAP that is named based on its location, has not been imaged by an efficient chemical tool in living cells. Considering the fact that ERAP1 is localized to the ER,[6] a novel ER-targeting TP fluorescent probe (**SNCL**) was designed and synthesized on the basis of an ICT mechanism. Simultaneously, **NCL** without an ER-targeting group was also synthesized as a control probe. In these two fluorescent probes, 4-hydroxy-1,8-naphthalimide was selected as the fluorophore due to its desirable photophysical properties. A tertiary carbamyl linkage with 1,2-diamine-based cyclization was chosen as the spacer owing to its stability toward spontaneous hydrolysis and quick response to aminopeptidases. In **SNCL**, a methyl sulfonamide moiety was selected as the ER-targeting group. When the pseudopeptide was cleaved by the target enzyme, the cyclic urea and the fluorophore (4-hydroxy-1,8-naphthalimide) were released to trigger a yellow fluorescent signal.

Photophysical Properties and Stability. Because ERAP1 is a LAP and shares the same substrates, we used LAP as the target in vitro. The spectral properties of **SNCL** (10 μM) were examined at 37 °C in a buffered aqueous DMSO solution (10 mM PBS, pH = 7.4, DMSO/H_2O = 1:19, v/v). As shown in Figure 1A, **SNCL** exhibited very weak fluorescence without LAP, but it showed a dramatic fluorescence enhancement at 550 nm with increasing concentrations of LAP. Meanwhile, the maximum absorption wavelength of **SNCL** changed from 347 to 445 nm upon the addition of LAP (Figure S1). These changes in the photophysical properties of **SNCL** were caused by an enzyme-triggered cleavage reaction, releasing the 4-hydroxy-1,8-naphthalimide fluorophore. A satisfactory linear relationship between the fluorescent signal intensity and the LAP concentration over a range from 5 to 40 U/L was also observed (Figure 1B inset), and the detection limit for LAP was calculated to be 0.21 U/L (3σ/slope). Such a detection limit was as low as that for previously reported LAP fluorescent probes,[46] indicating that **SNCL** was sensitive and capable of imaging intracellular LAP activity. Moreover, a strong specific interaction between **SNCL** and LAP was observed by measuring the Michaelis constant (K_m = 92.82 μM) (Figure S2). The fluorescence and absorption spectra of **NCL** in the absence and presence of LAP were also recorded under the same conditions (Figure S3).

In this study, the TP fluorescence properties of **SNCL** in the absence and presence of LAP were also investigated (Figure S4). The TP excitation cross-section of **SNCL** in the presence and absence of LAP were measured to be 92 and 13 GM at 820 nm, respectively. Under TP excitation at 820 nm, **SNCL** exhibited very weak fluorescence, but it showed strong fluorescence in the presence of LAP (Figure 1C), which suggested that **SNCL** could be used for TP fluorescence imaging.

As previously described, the unique linker used in **SNCL** not only minimized steric hindrance at the scissile bond, which contributed to the rapid response of **SNCL**, but also made **SNCL** stable in the absence of the target enzyme.[3] As shown in Figure 1D, in the absence of LAP, no obvious false positive signal by spontaneous hydrolysis was observed after 24 h in buffer solution (pH = 7.4), which meant that **SNCL** was stable and suitable for the detection of LAP in biosystems.

Selectivity Screening. The selectivity of **SNCL** to LAP was also investigated to determine whether **SNCL** was appropriate for use in complex biological systems. **SNCL** was treated with various potential interfering species. As shown in Figure 2A, other interfering species induced no obvious changes in the fluorescence intensity. Next, control experiments were performed in the presence of bestatin, an inhibitor of LAP, to further validate the selectivity of **SNCL**. As exhibited in Figure S5, weak fluorescence was observed in the control experiments. These results indicated that **SNCL** was selectively catalyzed by LAP and could be suitable for use in complex systems.

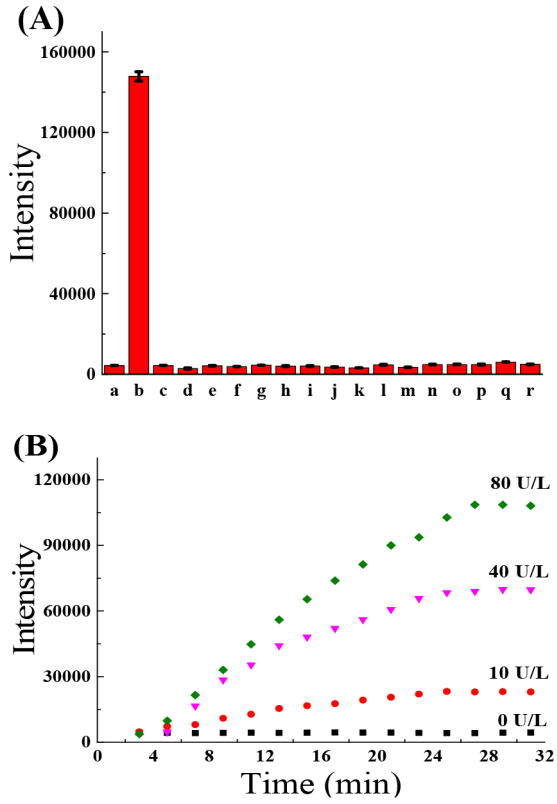

Figure 2. (A) Selectivity of **SNCL** (10 μM) toward various agents existing in human tissue: (a) blank, (b) LAP (100 U/L), (c) GGT (100 U/L), (d) β-galactosidase (100 U/L), (e) tyrosinase (100 U/L), (f) Cys (1 mM), (g) glucose (10 mM), (h) glycine (1 mM), (i) GSH (10 mM), (j) BSA (100 μM), (k) ascorbic acid (1 mM), (l) dithiothreitol (1 mM), (m) valine (1 mM), (n) H_2O_2 (50 μM), (o) NaClO (50 μM), (p) $MgCl_2$ (2.5 mM), (q) $CaCl_2$ (2.5 mM), and (r) *N*-ethylmaleimide (5 mM). (B) Fluorescence kinetic curves of LAP incubated with **SNCL** (10 μM) at different concentrations (0, 10, 40, or 80 U/L) under physiological conditions. $\lambda_{ex/em}$ = 420/550 nm.

Dynamic Response of SNCL to LAP. The effects of pH and temperature on the catalytic activity of LAP were explored before carrying out kinetic investigations (Figure S6 and S7). These results showed that the catalytic activity of LAP performed well under physiological conditions (pH = 7.4, *T* = 37 °C). Then, fluorescence kinetic curves of LAP reacting with **SNCL** at different concentrations (0, 10, 40, or 80 U/L) were recorded under physiological conditions (Figure 2B). In the absence of LAP, no obvious fluorescence change was observed in the tested system. However, the fluorescence intensity of **SNCL** increased rapidly when it was treated with different concentrations of LAP and reached a plateau after 30

DOI: 10.1021/acs.analchem.7b01561
Anal. Chem. 2017, 89, 7641−7648

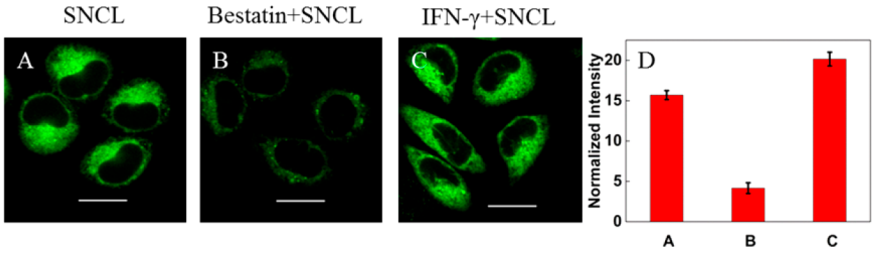

Figure 3. Fluorescence images of HeLa cells incubated with **SNCL** (10 μM) under different conditions. (A) HeLa cells incubated with **SNCL** for 30 min. (B) HeLa cells pretreated with bestatin (100 μM) for 30 min and then incubated with **SNCL** for another 30 min. (C) HeLa cells pretreated with IFN-γ (0.5 μg/mL) for 2 days and then incubated with **SNCL** for 30 min. (D) Relative fluorescence intensity of HeLa cells stained with **SNCL** in panels A–C. The images were collected at 470–540 nm upon excitation at 405 nm. Scale bar: 20 μm.

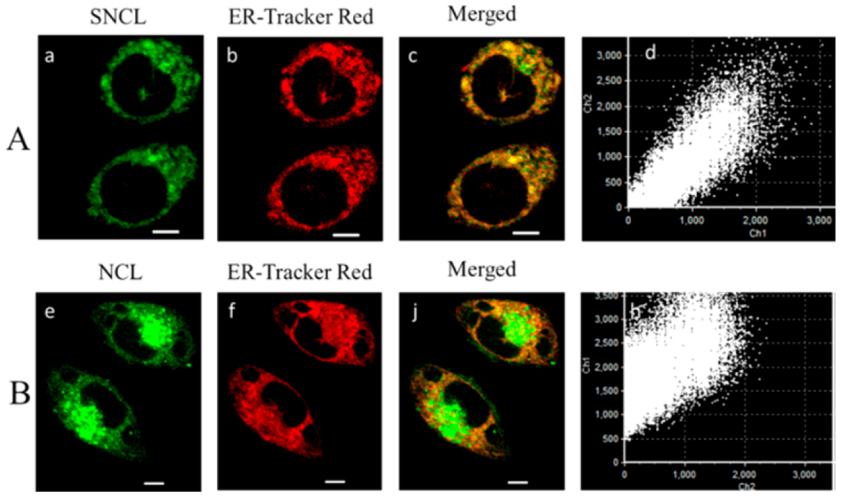

Figure 4. Colocalization test of (A) **SNCL** and (B) **NCL** to the ER. (a, e) Fluorescence images of **SNCL** and **NCL** (10 μM, λ_{ex} = 405 nm, λ_{em} = 470–540 nm) in HeLa cells, respectively. (b, f) Fluorescence image of ER-Tracker Red (0.5 μM, λ_{ex} = 543 nm, λ_{em} = 580–650 nm). (c, j) Overlay of panels (a) and (b) and panels (e) and (f), respectively. (d, h) Intensity correlation plot of the stain. Scale bar: 5 μm.

min. These results suggested that **SNCL** may offer the ability to image changes in LAP sensitively and rapidly.

Response Mechanism. To confirm the proposed mechanism (Scheme 1), UV–vis spectra of **SNCL** was recorded in the presence of LAP (Figure S8). Upon addition of LAP to **SNCL**, the absorption band at 347 nm decreased, along with the appearance of a new one at 445 nm (pH = 7.4), which was similar to the reaction product of **SNCL** with LAP. The reaction mixture was also analyzed by HPLC (Figure S9). When **SNCL** was incubated with LAP in buffer solution at 37 °C for 30 min, a new peak at 19.7 min was observed. It was suggested that the new peak belongs to the 4-hydroxy-1,8-naphthalimide fluorophore. These results demonstrated that **SNCL** was exclusively catalyzed by LAP and then converted to the 4-hydroxy-1,8-naphthalimide fluorophore.

Fluorescence Imaging of Endogenous ERAP1 Activity in HeLa Cells. Cell viability in the presence of **SNCL** or **NCL** was first examined by a standard CCK-8 assay with HeLa cells. As shown in Figure S10, **SNCL** and **NCL** both exhibited relatively low cytotoxicity to cultured cells.

Next, we further extended the potential application of **SNCL** to the cellular fluorescence imaging of ERAP1 activity. As shown in Figure 3A,B, HeLa cells incubated with **SNCL** for 30 min showed strong fluorescence, which decreased significantly in the presence of bestatin (100 μM), demonstrating the feasibility of **SNCL** to monitor ERAP1 in living cells. To further confirm that the intracellular fluorescence enhancement was indeed triggered by ERAP1, HeLa cells were pretreated with interferon-γ (IFN-γ) for 2 days and then incubated with **SNCL** for 30 min (Figure 3C). Previous studies have proved that IFN-γ induces an increase in ERAP1 content and does not affect other aminopeptidases in the ER.[4] As displayed in Figure 3D, the relative pixel intensity of HeLa cells preincubated with IFN-γ was higher than that of the control group without IFN-γ under the same fluorescence imaging conditions.

Subcellular Distribution of ERAP1. Having imaged ERAP1 in living cells, the subcellular distribution of ERAP1 was further studied by conducting colocalization experiments in HeLa cells. The cells were pretreated with 10 μM **SNCL** or **NCL** for 30 min before incubation with 0.5 μM ER-Tracker Red for 20 min. As displayed in Figure 4A, the fluorescence of **SNCL** overlapped well with that of ER-Tracker Red, a commercial ER-specific dye, with an overlap coefficient of 0.91. However, under the same conditions, the distribution of **NCL** in HeLa cells showed a rather poor correspondence, with an overlap coefficient of 0.71 (Figure 4B), which further verified the organelle-specific trap of **SNCL** in the ER. Moreover, a real-time imaging experiment was also performed. As shown in Figure S11, **SNCL** could quickly localize to the ER within 3 min, and the cells displayed gradually enhanced fluorescence within 30 min with no obvious fluorescence changes observed in the cytoplasm, which demonstrated that the enzyme-catalyzed reaction occurred in the ER. These results all show that **SNCL** can serve as an efficient fluorescent probe for imaging endogenous ERAP1 in living cells without cell damage. These unique properties of **SNCL** also inspired us

DOI: 10.1021/acs.analchem.7b01561
Anal. Chem. 2017, 89, 7641–7648

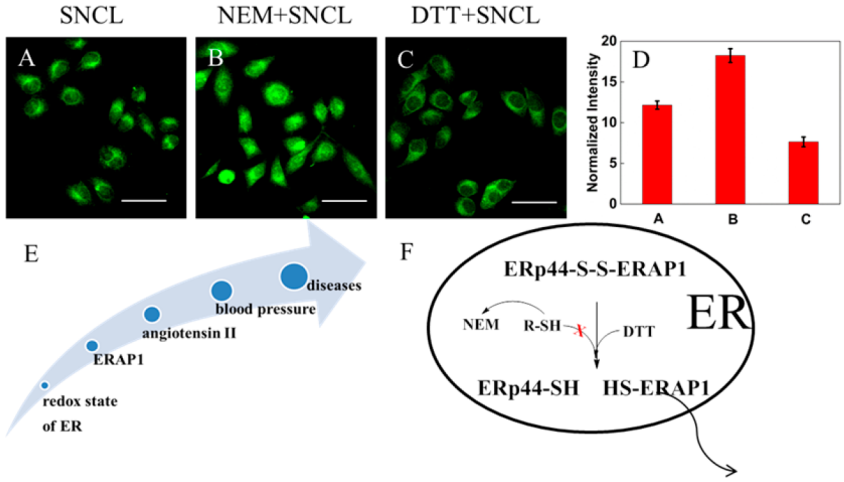

Figure 5. Fluorescence images of **SNCL** (10 μM) in HeLa cells under different conditions. (A) Cells were incubated with **SNCL** for 30 min. (B) Cells were pretreated with NEM (5 mM) for 1 h and then incubated with **SNCL** for 30 min. (C) Cells were pretreated with DTT (10 mM) for 20 min and then incubated with **SNCL** for 30 min. (D) Relative fluorescence intensity of HeLa cells stained with **SNCL** in panels A–C. (E) Relationship between ER redox state and diseases. (F) Redox-regulated disulfide bond between ERp44 and ERAP1. The images were collected at 470–540 nm upon excitation at 405 nm. Scale bar: 50 μm.

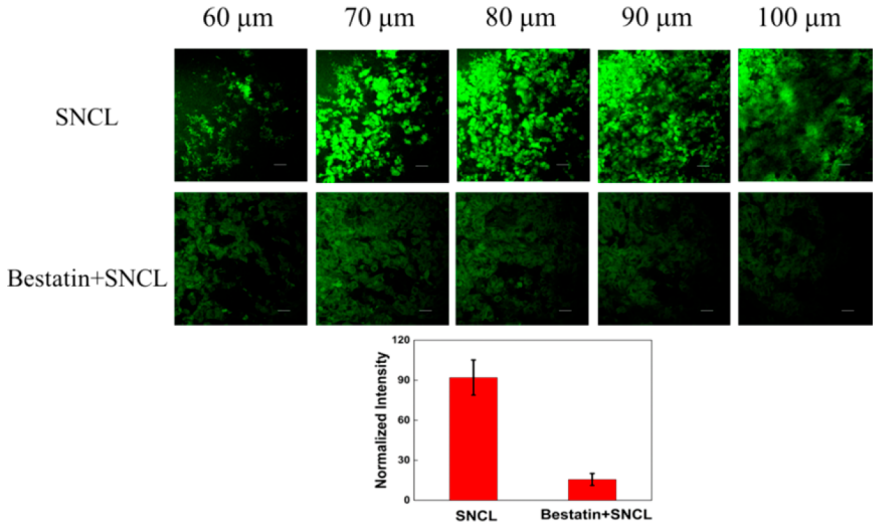

Figure 6. Two-photon microscopy images of HeLa tumor tissue at different depths with magnification at 60× under different conditions. The images were collected at 470–540 nm upon excitation at 820 nm. Scale bar: 20 μm.

to explore some ERAP1-related physiological processes in living cells.

Fluorescence Imaging of ERAP1 under Different ER Redox States. As mentioned above, blood pressure is maintained through the cleavage of angiotensin II by ERAP1. Studies revealed that the ER redox state regulates serum angiotensin II levels via controlling the release of ERAP1 from the ER to the serum.[8] The process is depicted in Figure 5E. In this part, **SNCL** was expected to monitor changes in ERAP1 content under altered ER redox conditions. *N*-Ethylmaleimide (NEM), an inhibitor of intermolecular thiol–disulfide exchange, and dithiothreitol (DTT), a reductant that inhibits disulfide bond formation, were employed to gain insight into the influence of the redox state of the ER on the release of ERAP1 (Figure 5F). As shown in Figure 5B, the cells pretreated with NEM exhibited stronger fluorescence than those without NEM. In contrast, cells pretreated with DTT displayed weaker fluorescence than those without DTT (Figure 5C). The relative fluorescence intensities of HeLa cells stained with **SNCL** under different conditions are displayed in Figure 5D. These results demonstrated that **SNCL** can be used to sense disturbances in the redox state of the ER by measuring ERAP1 activity. Thus, we believe that some cardiovascular diseases induced by disturbances in the redox state of the ER can be diagnosed by using **SNCL** as an ERAP1 sensor.

Next, TP confocal fluorescence microscopy was adopted to examine the feasibility of using **SNCL** for imaging endogenous ERAP1. As shown in Figure S12, bright fluorescence was observed from **SNCL** when it was excited at 820 nm, which revealed that **SNCL** is practical for use in TP fluorescence imaging. Furthermore, the photostability of **SNCL** in HeLa cells was studied by TP confocal fluorescence microscopy. After being incubated with **SNCL** for 30 min, HeLa cells were irradiated at 820 nm for 30 min, and the signal intensity in the 470–540 channel showed no obvious changes (Figure S13B), indicating the high photostability of **SNCL**.

Two-Photon Fluorescence Imaging of ERAP1 Activity in Tumor Tissue. After the study in living cells, we performed

DOI: 10.1021/acs.analchem.7b01561
Anal. Chem. 2017, 89, 7641–7648

TP fluorescence imaging of this probe in HeLa tumor tissues. Tumor tissues were incubated with 50 μM **SNCL** at 37 °C for 1 h and then imaged. Under TP excitation, a strong fluorescence response was observed at a depth of 50−120 μm (Figure S14), which demonstrated that **SNCL** is capable of imaging endogenous ERAP1 deep in a tissue. A control sample, which was pretreated with 2 mM bestatin before incubation with 50 μM **SNCL**, showed weaker fluorescence at a depth of 60−100 μm (Figure 6). These results indicated that **SNCL** can be used to image ERAP1 activity in tumor tissue. Simultaneously, one-photon fluorescence imaging of ERAP1 in tumor tissue was also carried out, and the penetration depth of the signal reached only from 50 to 70 μm (Figure S14). These results confirmed that TP fluorescence imaging using **SNCL** has more advantages than one-photon imaging and that **SNCL** can be used for imaging ERAP1 in tissues under TP excitation.

CONCLUSIONS

In summary, a stable ER-targeting TP fluorescent probe (**SNCL**) was synthesized and applied to monitor ERAP1 activity in living cells and tissues. We found that **SNCL** can be used to monitor alterations in ERAP1 in living cells under different conditions. Treating HeLa cells with IFN-γ increased the amount of ERAP1, which could be detected by **SNCL**. Moreover, after incubation of HeLa cells with NEM or DTT, **SNCL** was able to sense the disturbance in the ER by imaging the activity of ERAP1. Finally, **SNCL** was successfully applied for TP imaging of ERAP1 in tumor tissue at a depth of 50−120 μm. In the future, **SNCL** is expected to be used in the diagnosis of ERAP1-related diseases.

ASSOCIATED CONTENT

Supporting Information

The Supporting Information is available free of charge on the ACS Publications website at DOI: 10.1021/acs.analchem.7b01561.

Synthesis details and spectroscopic data (PDF)

AUTHOR INFORMATION

Corresponding Authors

*E-mail: syhuan@hnu.edu.cn (S.-Y.H.).
*E-mail: fengliquhn@hotmail.com (F.-L.Q.).
*E-mail: xbzhang@hnu.edu.cn (X.-B.Z.).

ORCID

Lin Yuan: 0000-0002-1015-5319
Xiao-Bing Zhang: 0000-0002-4010-0028
Weihong Tan: 0000-0002-8066-1524

Author Contributions

§S.X. and H.-W.L. contributed equally to this work.

Notes

The authors declare no competing financial interest.

ACKNOWLEDGMENTS

This work was supported by the NSFC (Grants 21675043, 21325520, 21327009, and J1210040), the Foundation for Innovative Research Groups of NSFC (Grant 21521063), and the Science and Technology Project of Hunan Province (2016RS2009 and 2016WK2002).

REFERENCES

(1) Hattori, A.; Matsumoto, H.; Mizutani, S.; Tsujimoto, M. *J. Biochem.* **1999**, *125*, 931−938.
(2) Hattori, A.; Matsumoto, H.; Mizutani, S.; Tsujimoto, M. *J. Biochem.* **2001**, *130*, 235−241.
(3) Schomburg, L.; Kollmus, H.; Friedrichsen, S.; Bauer, K. *Eur. J. Biochem.* **2000**, *267*, 3198−3207.
(4) Saric, T.; Chang, S. C.; Hattori, A.; York, I. A.; Markant, S.; Rock, K. L.; Tsujimoto, M.; Goldberg, A. L. *Nat. Immunol.* **2002**, *3*, 1169−1176.
(5) Hammer, G. E.; Gonzalez, F.; Champsaur, M.; Cado, D.; Shastri, N. *Nat. Immunol.* **2006**, *7*, 103−112.
(6) Shastri, N.; Schwab, S.; Serwold, T. *Annu. Rev. Immunol.* **2002**, *20*, 463−493.
(7) Fruci, D.; Ferracuti, S.; Limongi, M. Z.; Cunsolo, V.; Giorda, E.; Fraioli, R.; Sibilio, L.; Carroll, O.; Hattori, A.; van Endert, P. M.; Giacomini, P. *J. Immunol.* **2006**, *176*, 4869−4879.
(8) Hisatsune, C.; Ebisui, E.; Usui, M.; Ogawa, N.; Suzuki, A.; Mataga, N.; Takahashi-Iwanaga, H.; Mikoshiba, K. *Mol. Cell* **2015**, *58*, 1015−1027.
(9) Zhang, H.; Fan, J.; Wang, J.; Dou, B.; Zhou, F.; Cao, J.; Qu, J.; Cao, Z.; Zhao, W.; Peng, X. *J. Am. Chem. Soc.* **2013**, *135*, 17469−17475.
(10) Dai, Z. R.; Ge, G. B.; Feng, L.; Ning, J.; Hu, L. H.; Jin, Q.; Wang, D. D.; Lv, X.; Dou, T. Y.; Cui, J. N.; Yang, L. *J. Am. Chem. Soc.* **2015**, *137*, 14488−14495.
(11) Zhang, J.; Liu, H. W.; Hu, X. X.; Li, J.; Liang, L. H.; Zhang, X. B.; Tan, W. *Anal. Chem.* **2015**, *87*, 11832−11839.
(12) Xu, W.; Zeng, Z. B.; Jiang, J. H.; Chang, Y. T.; Yuan, L. *Angew. Chem., Int. Ed.* **2016**, *55*, 13658−13699.
(13) Denk, W.; Strickler, J. H.; Webb, W. W. *Science* **1990**, *248*, 73−76.
(14) Kim, H. M.; Cho, B. R. *Chem. Rev.* **2015**, *115*, 5014−5055.
(15) Helmchen, F.; Denk, W. *Nat. Methods* **2005**, *2*, 932−940.
(16) Liu, H. W.; Liu, Y.; Wang, P.; Zhang, X. B. *Methods Appl. Fluoresc.* **2017**, *5*, 012003.
(17) Zhu, B.; Li, P.; Shu, W.; Wang, X.; Liu, C.; Wang, Y.; Wang, Z.; Wang, Y.; Tang, B. *Anal. Chem.* **2016**, *88*, 12532−12538.
(18) Cheng, D.; Pan, Y.; Wang, L.; Zeng, Z. B.; Yuan, L.; Zhang, X. B.; Chang, Y. T. *J. Am. Chem. Soc.* **2017**, *139*, 285−292.
(19) Zhou, S. S.; Xue, X.; Jiang, B.; Tian, Y. P. *Sci. China: Chem.* **2012**, *55*, 334−340.
(20) Shu, Y.; Liu, W. *Sci. China: Chem.* **2016**, *59*, 436−441.
(21) Mao, Z.; Hu, L.; Dong, X.; Zhong, C.; Liu, B. F.; Liu, Z. *Anal. Chem.* **2014**, *86*, 6548−6554.
(22) Tang, Y.; Kong, X.; Xu, A.; Dong, B.; Lin, W. *Angew. Chem., Int. Ed.* **2016**, *55*, 3356−3359.
(23) Ustione, A.; Piston, D. W. *J. Microsc.* **2011**, *243*, 221−226.
(24) Patterson, G. H.; Piston, D. W. *Biophys. J.* **2000**, *78*, 2159−2162.
(25) Kim, H. M.; Cho, B. R. *Acc. Chem. Res.* **2009**, *42*, 863−872.
(26) Zhang, L.; Duan, D.; Liu, Y.; Ge, C.; Cui, X.; Sun, J.; Fang, J. *J. Am. Chem. Soc.* **2014**, *136*, 226−233.
(27) Zhu, B.; Gao, C.; Zhao, Y.; Liu, C.; Li, Y.; Wei, Q.; Ma, Z.; Du, B.; Zhang, X. *Chem. Commun.* **2011**, *47*, 8656−8658.
(28) Zhu, B.; Guo, B.; Zhao, Y.; Zhang, B.; Du, B. *Biosens. Bioelectron.* **2014**, *55*, 72−75.
(29) Tran, T. M.; Colbert, R. A. *Curr. Opin. Rheumatol.* **2015**, *27*, 357−363.
(30) Mcmahon, B. K.; Pal, R.; Parker, D. *Chem. Commun.* **2013**, *49*, 5363−5365.
(31) Xiao, H.; Li, P.; Hu, X.; Shi, X.; Zhang, W.; Tang, B. *Chem. Sci.* **2016**, *7*, 6153−6159.
(32) Christenson, I.; Persson, K.; Thorkilsen, B.; Halvarson, H.; Nilsson, L. *Acta Chem. Scand.* **1964**, *18*, 904−922.
(33) Hegarty, A. F.; Frost, L. N.; Coy, J. H. *J. Org. Chem.* **1974**, *39*, 1089−1093.
(34) Thorn-Seshold, O.; Vargas-Sanchez, M.; Mckeon, S.; Hasserodt, J. *Chem. Commun.* **2012**, *48*, 6253−6255.

DOI: 10.1021/acs.analchem.7b01561
Anal. Chem. 2017, 89, 7641−7648

(35) Prost, M.; Canaple, L.; Samarut, J.; Hasserodt, J. *ChemBioChem* **2014**, *15*, 1413−1417.
(36) Mao, G. J.; Wei, T. T.; Wang, X. X.; Huan, S.; Lu, D. Q.; Zhang, J.; Zhang, X. B.; Tan, W.; Shen, G. L.; Yu, R. Q. *Anal. Chem.* **2013**, *85*, 7875−7881.
(37) Makarov, N. S.; Drobizhev, M.; Rebane, A. *Opt. Express* **2008**, *16*, 4029−4047.
(38) Gu, K.; Liu, Y.; Guo, Z.; Lian, C.; Yan, C.; Shi, P.; Tian, H.; Zhu, W. H. *ACS Appl. Mater. Interfaces* **2016**, *8*, 26622−26629.
(39) Gong, Q.; Shi, W.; Li, L.; Ma, H. *Chem. Sci.* **2016**, *7*, 788−792.
(40) Huang, H.; Tanaka, H.; Hammock, B. D.; Morisseau, C. *Anal. Biochem.* **2009**, *391*, 11−16.
(41) Yoon, H. Y.; Shim, S. H.; Baek, L. J.; Hong, J. I. *Bioorg. Med. Chem. Lett.* **2011**, *21*, 2403−2405.
(42) Kushida, Y.; Hanaoka, K.; Komatsu, T.; Terai, T.; Ueno, T.; Yoshida, K.; Uchiyama, M.; Nagano, T. *Bioorg. Med. Chem. Lett.* **2012**, *22*, 3908−3911.
(43) Ho, N. H.; Weissleder, R.; Tung, C. H. *Tetrahedron* **2006**, *62*, 578−585.
(44) Koji, S.; Takamitsu, S.; Toshihiko, N.; Tetsuo, T.; Yuichi, K. *Clin. Chim. Acta* **1978**, *84*, 85−91.
(45) Zhang, X. B.; Waibel, M.; Hasserodt, J. *Chem. - Eur. J.* **2010**, *16*, 792−795.
(46) He, X.; Li, L.; Fang, Y.; Shi, W.; Li, X.; Ma, H. *Chem. Sci.* **2017**, *8*, 3479.

DOI: 10.1021/acs.analchem.7b01561
Anal. Chem. 2017, 89, 7641−7648